# Miscibility, Intermolecular Interactions, and Thermal Behavior of Poly(hydroxy ether of Bisphenol A)/Poly(ethyl oxazoline) Blends

**Cheryl Lau, Sixun Zheng, Zhikai Zhong, and Yongli Mi***

*Department of Chemical Engineering, The Hong Kong University of Science and Technology, Clear Water Bay, Kowloon, Hong Kong*

*Received May 6, 1998; Revised Manuscript Received August 19, 1998*

ABSTRACT: The miscibility, intermolecular interactions and thermal behavior of the poly(hydroxy ether of Bisphenol A) (Phenoxy)/poly(ethyl oxazoline) (PEOx) blends were investigated by differential scanning calorimetry (DSC), Fourier transform infrared spectroscopy (FTIR), and high-resolution solid-state nuclear magnetic resonance (NMR) spectroscopy. Each composition of the Phenoxy/PEOx blends investigated displays a single glass transition temperature ($T_g$), which is intermediate between those of the pure components and regularly varies with blend composition. The results of FTIR showed that there are intermolecular interactions between the pendant hydroxyl groups of Phenoxy and the carbonyl groups of PEOx. Spin−lattice relaxation times in both the laboratory and the rotating frame determined by high-resolution solid state $^{13}C$ NMR spectroscopy reveal that the spin-diffusion among all protons in the blends averages out the whole relaxation process, suggesting that the blends are intimately mixed on the scale of 10−15 Å.

## Introduction

In the past decades, polymer blends have received more and more attention because they can offer a wide range of material properties. Since the physical properties of such blends are strongly influenced by the miscibility, there is a growing interest in studying miscibility and phase behavior. Various techniques have been successfully employed to investigate the miscibility of polymer blends, such as thermal analysis, mechanical testing, light scattering, microscopy, and spectroscopy methods.[1,2] Among the spectroscopic techniques, Fourier transform infrared spectroscopy and high-resolution solid-state nuclear magnetic resonance (NMR) spectroscopy are powerful techniques for determining the scale of miscibility and for studying the morphology and the intermolecular interactions of polymer blends.[3−5]

Poly(hydroxy ether of Bisphenol A) (Phenoxy) is an amorphous polymer which can be miscible with proton-accepting polymers through the formation of hydrogen bonding.[6−12] Poly(ethyl oxazoline) (PEOx), a tertiary amide amorphous polymer with a glass-transition temperature ($T_g$) of 57 °C, has been reported to be miscible with a wide variety of other polymers.[13−16]

J. Dai et al. reported the complexation behavior of poly(hydroxy ether of Bisphenol A) with three tertiary amide polymers, namely, poly(*N*-methyl-*N*-vinylacetamide) (PMVAc), poly(*N*,*N*-dimethylacrylamide) (PDMA), and PEOx, and they found that complexation between Phenoxy and PEOx did not occur upon mixing.[13] We, therefore, wish to carry on this study by exploring the scale of interchain miscibility using a high-resolution solid-state NMR technique. DSC and FTIR results are also reported in this study as a necessary supplement because the literature data were obtained under different experimental conditions.[14−16]

Traditionally, the observation of a single glass transition temperature ($T_g$) in a blend is used to assert the miscibility on the scale of 100−300 Å.[2,32] Here, the study of miscibility in the Phenoxy/PEOx blends is focused on a smaller scale using high-resolution solid-state NMR technique because the length-scale detected in this technique can be down to 20−30 Å in the measurements of the proton spin−lattice relaxation times in the rotating frame, $T_{1\rho}(H)$. The Phenoxy/PEOx blends with a wide range of different compositions were prepared and the miscibility and intermolecular interactions of this system were investigated by determining $^{13}C$ solid-state NMR spectra, the proton spin−lattice relaxation time in the laboratory frame, $T_1(H)$, and that in the rotating frame, $T_{1\rho}(H)$, using high-resolution solid-state NMR. In addition, the miscibility, intermolecular interactions, and thermal behavior were also studied by DSC and FTIR.

## Experimental Section

**Materials and Samples Preparation.** Phenoxy used in this study was purchased from Scientific Polymer Products, Inc., and it has a weight-average molecular weight ($M_w$) of 85 000. The PEOx with a weight-average molecular weight ($M_w$) of 500 000 was obtained from Polysciences, Inc. Phenoxy/PEOx blends were prepared according to the following composition (w/w): 100/0, 90/10, 70/30, 50/50, 30/70, 10/90, 0/100. Films of pure polymers and their blends were prepared by solution casting using chloroform ($CHCl_3$) as a common solvent. Most solvent was removed at ambient temperature. To further remove residual solvent, all the blend films were dried under vacuum at 55 °C for 2 weeks.

The thin films of samples for FTIR analysis were prepared by casting the $CHCl_3$ solutions onto NaCl windows; the casting process was carried out at 55 °C. The films were dried at 55 °C in a vacuum oven. All films were sufficiently thin to be within the absorbance range where the Lambert−Beer law is obeyed.

**Differential Scanning Calorimetry.** The calorimetric measurement were conducted on a Perkin-Elmer Pyris 1 differential scanning calorimeter in a dry nitrogen atmosphere. The instrument was calibrated with Indium and Zinc standards for temperature and energy. For both pure polymers and their blends, samples were first scanned from 0 to 150 °C at 10 °C/min, followed by quenching to 0 °C, and rescanned to 150 °C at 10 °C/min. The values of $T_g$ were taken as the midpoint of the heat capacity transition.

* To whom all correspondence should be addressed.

10.1021/ma980714i CCC: $15.00 
Published on Web 09/30/1998

**Fourier Transform Infrared Spectroscopy.** Infrared spectra were recorded on a Bomem MB104 Fourier transform infrared spectrometer in order to investigate intermolecular interactions. All spectra were obtained at room temperature with a resolution of 2 $cm^{-1}$ and were signal averaged over 64 scans.

**High-Resolution $^{13}C$ Solid-State NMR Spectroscopy.** High-resolution solid-state NMR experiments were carried out at room temperature (27 °C) on a JEOL EX-400 FT NMR spectrometer at the resonance frequencies of 399.65 MHz for proton and 100.40 MHz for carbon-13. High-resolution $^{13}C$ solid-state NMR spectra were obtained using the cross polarization (CP)/magic angle spinning (MAS)/high-power dipolar decoupling (DD) technique. A $^1H$ 90° pulse width of 5.5 $\mu$s was employed with free induction decay (FID) signal accumulation. The Hartmann−Hahn CP matching and dipolar decoupling field was 40 kHz, and total sideband suppression (TOSS) pulse sequence was used for suppressing spinning sidebands. The rate of MAS was 4.9−5.1 kHz for measuring $^{13}C$ spectra and relaxation times. The CP Hartmann−Hahn contact time was set at 1.5 ms to observe the spectra of the pure components and their blends, 1024 scans were used for the signal accumulation in obtaining the $^{13}C$ spectra, and 512 scans were used for relaxation times measurements. In all experiments, a recycle delay of 12 s was used to ensure that the net magnetization was completely relaxed after each cycle. The chemical shifts of all $^{13}C$ spectra were calibrated in parts per million using the $^{13}C$ of the methine carbon of solid adamantane (29.5 ppm) relative to TMS as an external reference standard.

Proton spin−lattice relaxation times in the laboratory frame, $T_1(H)$, were measured by monitoring the decay of specific carbon resonance intensities after the $^1H$ $180^o-\tau-90^o$ pulse sequence using the inversion−recovery (IR) method. Proton spin−lattice relaxation times in the rotating frame, $T_{1\rho}(H)$, were determined by monitoring the cross polarized $^{13}C$ signal intensities after a $^1H$ matched spin-lock pulse sequence.

The pulse sequences used for the high-resolution solid-state NMR experiments are shown in Figure 1.

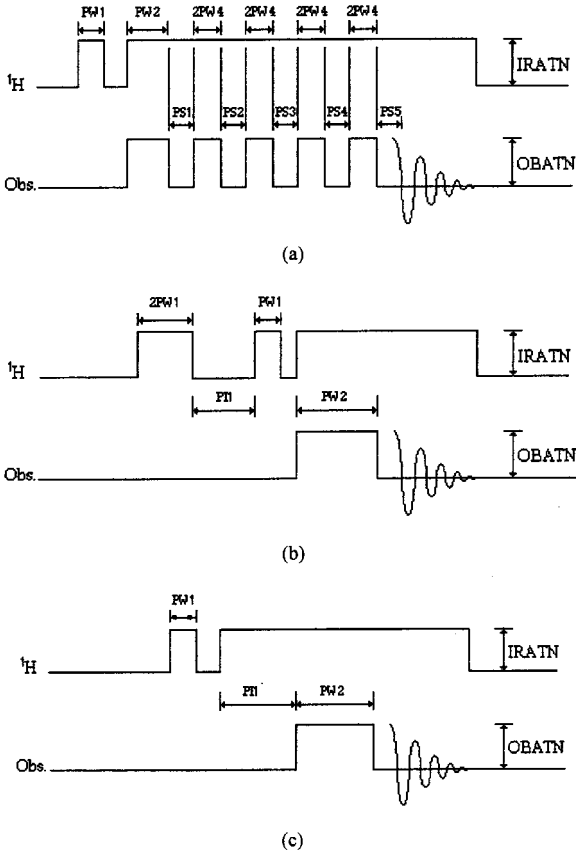


**Figure 1.** Pulse sequences used in NMR measurements: (a) sequence for $^{13}C$ CP/MAS/DD spectra measurement with TOSS; (b) sequence for $T_1(H)$ measurement; (c) sequence for $T_{1\rho}(H)$ measurement. Key: PW1, 90° pulse of $^1H$; PW2, contact time; PW4, 90° pulse of $^{13}C$; PI1, delay time; PS1−5, time interval.

## Results and Discussion

**Differential Scanning Calorimetry.** All the Phenoxy/PEOx blend films cast from $CHCl_3$ were transparent at room temperature, suggesting the absence of phase separation in the blends on the scale exceeding the wavelength of the visible light. The Phenoxy/PEOx blends were then subjected to DSC measurements. The DSC thermograms are shown in Figure 2, and the results are summarized in Table 1. From Figure 2, it can be seen that all the Phenoxy/PEOx blends exhibit a single glass transition temperature ($T_g$) and the $T_g$s of the blends lie between those of the pure components. The appearance of a single and composition-dependent $T_g$ for the Phenoxy/PEOx blends indicates that the blends exhibit a homogeneous amorphous phase on the dimensional scale to which DSC is sensitive.[2,32]

The $T_g$s obtained from Figure 2 were plotted vs blend composition in Figure 3. It can be seen that the $T_g$s of the blends with higher Phenoxy content are above the composition average line while those of blends with higher PEOx content fall below the composition average line. The $T_g$-composition data can be best-fitted by a S-shaped curve which suggests the presence of strong intermolecular interactions between Phenoxy and PEOx in the blends. It should be noted that the $T_g$ values are somewhat different from the previous published values,[13] perhaps because the sample preparation, experimental conditions, and instrumentation are not necessarily the same. However, the results of this study are

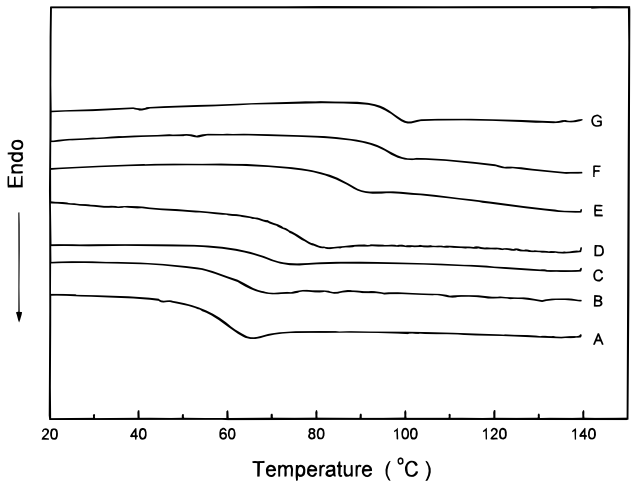


**Figure 2.** Second scan of DSC thermograms of the Phenoxy/PEOx blends: (A) 0, (B) 10, (C) 30, (D) 50, (E) 70, (F) 90, or (G) 100 wt % Phenoxy.

consistent with the previous work,[13] indicating that Phenoxy is completely miscible with PEOx over the entire composition range on the DSC scale.

**Fourier Transform Infrared Spectroscopy (FTIR).** In view of the chemical structures involved, it is believed that specific intermolecular interactions can occur in the blends. Fourier transform infrared spectroscopy is one of the most powerful tools for the identification and investigation of hydrogen bonding in polymers.

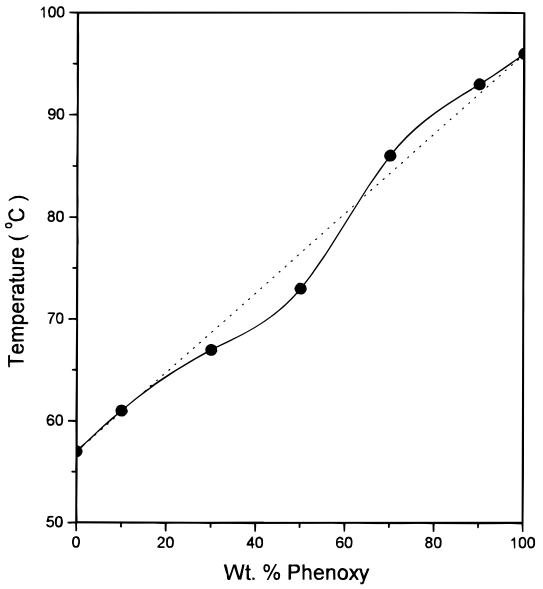


**Figure 3.** Plot of $T_g$ vs the composition of the Phenoxy/PEOx blends.

**Table 1. Glass Transition Temperature of Phenoxy, PEOx, and Their Blends from DSC Thermograms**

| composition (Phenoxy wt %) | glass transition temp ($T_g$) (°C) |
|---|---|
| 0 | 57 |
| 10 | 61 |
| 30 | 67 |
| 50 | 73 |
| 70 | 86 |
| 90 | 93 |
| 100 | 96 |

PEOx is a tertiary amide polymer in which the amide group is a proton acceptor and, therefore, there are two possible hydrogen bonding sites for PEOx to Phenoxy hydroxyl groups, namely, the carbonyl oxygen and the tertiary amide nitrogen atom. Studies from model compounds have shown that the association favors the former.[17,18] The absorption band, centered at 1640 $cm^{-1}$, is called amide I and is a combined mode with contribution of >C═O and C−N stretch, with a greater contribution from the former.[19] Owing to this combination mode, this band occurred at a lower wavenumber than expected for pure ester carbonyl band. In this study, we will refer this band as the carbonyl band of PEOx.

The FTIR spectra in the carbonyl stretching region for Phenoxy/PEOx blends are shown in Figure 4. Addition of Phenoxy results in a new band around 1610 $cm^{-1}$, which is assigned to PEOx hydrogen-bonded carbonyl groups. Its relative intensity depends on composition; the higher the Phenoxy content in the blend, the stronger the intensity of the associated PEOx band relative to that of the nonassociated one. Moreover, as the Phenoxy content increases in the blends, the nonassociated band shifts to the lower wavenumbers. The less double bond character the >C═O group has, the smaller the force constant of the bond and thus the lower the wavenumber at which the band occurs. Since the PEOx carbonyl group is hydrogen bonded to the Phenoxy hydroxyl group, its double bond character decreases and the absorption band shifts to the lower wavenumbers. Moreover, the chemical shift, $\Delta\nu = 30\ cm^{-1}$, indicates that the hydrogen bonding is rather strong. This result is consistent with the DSC

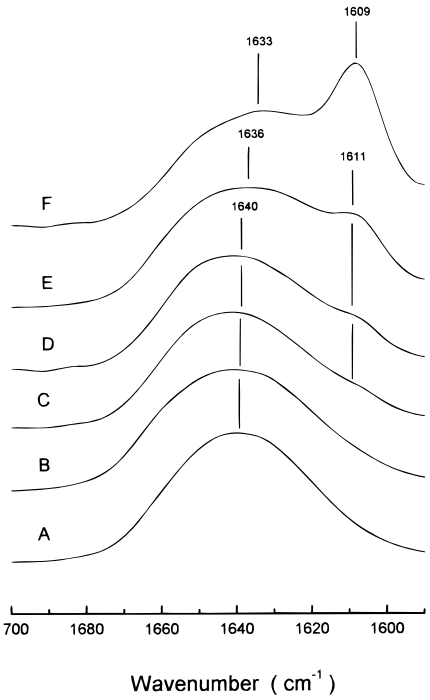


**Figure 4.** FTIR spectra in the carbonyl region of the Phenoxy/PEOx blends: (A) 0, (B) 10, (C) 30, (D) 50, (E) 70, or (F) 90 wt % Phenoxy.

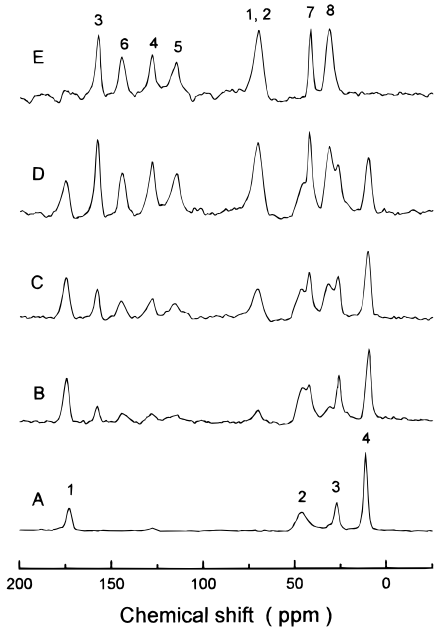


**Figure 5.** $^{13}C$ CP/MAS/DD spectra of the Phenoxy/PEOx blends: (A) 0, (B) 10, (C) 30, (D) 50, (E) 70, (F) 90, or (G) 100 wt % Phenoxy.

results in the way that the composition dependent $T_g$s fulfills an S-shaped curve which is also an indication of strong intermolecular hydrogen bond formation.

**$^{13}C$ CP/MAS/DD Solid-State NMR Spectra.** To ascertain the miscibility of Phenoxy/PEOx blends at the molecular level, high-resolution solid-state NMR was applied to probe the miscibility scale of the blends. $^{13}C$ CP/MAS/DD spectra of Phenoxy, PEOx, and their blends are shown in Figure 5. Phenoxy has seven resonance lines. The structure and peak assignment of Phenoxy are given as follows:[20]

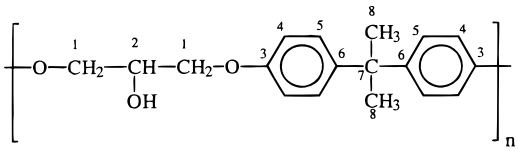

Poly(hydroxy ether of bisphenol A) (Phenoxy)

Four resonance peaks are observed in the $^{13}C$ NMR spectrum of the pure PEOx and are assigned as follows:

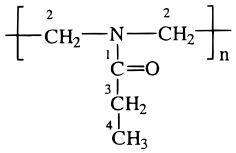

Poly(ethyl oxazoline) (PEOx)

It has been reported that there will be a change in the chemical shift and line width of the correlative carbon if significant interactions exist between the components in the blend.[21−23] If the carbonyl carbon resonance (174 ppm) is examined, it is found that there is only a slight downfield shift of chemical shift by about 0.7 ppm; however, there is an abrupt increase from 293 to 515 Hz in line width when the Phenoxy content is 70 wt % in the blend. In pure PEOx, the carbon of the nonassociated carbonyl resonates at 174 ppm; with an addition of Phenoxy to the system, intermolecular hydrogen bonding forms between the amide of PEOx and the pendant hydroxyls of Phenoxy. Obviously, the hydrogen-bonded carbonyl carbon resonates at a downfield with respect to the free carbonyl group; therefore, the increase in line width can be ascribed to the overlapping of resonances of the free and hydrogen-bonded carbonyl carbons. The results (Figure 6) are consistent with the DSC and FTIR results, indicating the formation of hydrogen bonding.

From the spectra of the blends, it is observed that the relative intensities of the resonance peaks change with the blend composition. The intensity of the Phenoxy resonance line becomes weaker in PEOx-rich blends and so does that of PEOx in Phenoxy-rich blends.

The relative intensity of the carbonyl peak (174 ppm) with respect to the intensity of the carbon resonance at 10 ppm is plotted as a function of Phenoxy content in Figure 7. It is expected that as PEOx content decreases, the intensity of this peak also decreases. However, it is found that there is a sharp increase (31−58%) in its intensity with addition of Phenoxy. It is believed that the increase of intensity is due to the formation of hydrogen bonding with the carbonyl group. Since the carbonyl carbon is nonprotonated, it experiences cross polarization much more slowly because of the weaker carbon−proton dipolar interaction, which involves protons attached to the neighboring atom. When it is hydrogen bonded to the hydroxyl group of Phenoxy, the hydroxyl proton has close contact with the carbonyl oxygen of PEOx, which can be considered as a source of the $^{1}H-^{13}C$ magnetization transfer. These intermolecular cross polarization effects cause a faster enhancement and, consequently, the observed intensity increase. Similar phenomena have been reported for miscible blends such as poly(vinyl alcohol)/poly(vinyl pyrrolidone) [21] and deuterated polystyrene/poly(vinyl methyl ether).[24]

**Proton Spin−Lattice Relaxation Time.** For the miscible polymer blends at the molecular scale, the protons of different chemical chains can be closely coupled and relax at an identical rate through the spin−diffusion mechanism, while protons far apart or in different environments relax at an independent rate. Therefore, the miscibility of a polymer blend can be investigated by the relaxation rates of protons corresponding to the polymer components.

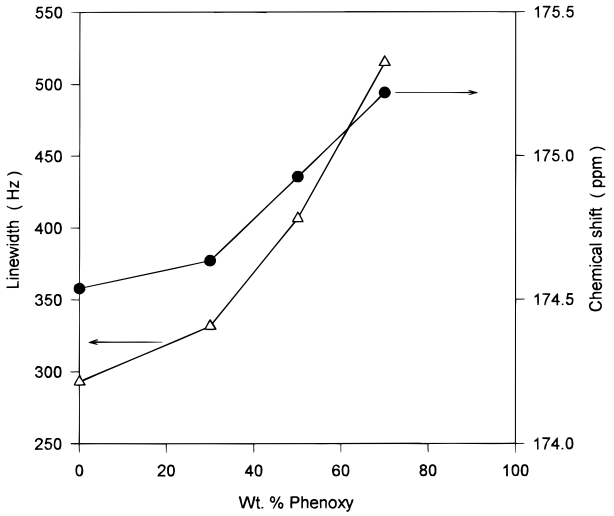


**Figure 6.** Plot of line width and chemical shift of carbonyl peak (174 ppm) of PEOx vs composition.

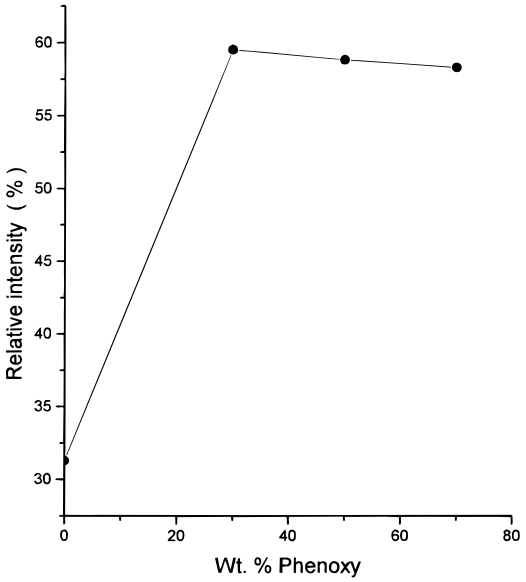


**Figure 7.** Plot of intensity ratio of carbonyl peak (174 ppm) and methyl peak (10 ppm) of PEOx vs composition.

The signal intensity of cross polarization depends on several competing processes, including the build up of intensity from carbon−proton cross polarization and the decay of proton and carbon signals. Contact time is the time which governs the magnetization transfer from proton to carbon. If the contact time is too short, only those protonated carbons such as $CH_3$ and $CH_2$ can be revealed because only a short contact time is enough for them to achieve full enhancement. For those nonprotonated carbons, enhancement is slow and takes a longer time. However, if the contact time is too long, the signals will decay away. Therefore, it is important to choose a suitable contact time for each system. $^{13}C$ solid-state NMR spectra of PEOx, determined as a function of cross polarization contact time, showed that peak intensity reaches its maximum at 2 ms, which

**Table 2. $T_1$ ($H$) Values (s) for Phenoxy, PEOx and Their Blends [a]**

| composition | PEOx | Phenoxy (PH) | | | | | PEOx | PH | | PEOx | |
|---|---|---|---|---|---|---|---|---|---|---|---|
| (PEOx wt %) | 174 ppm | 157 ppm | 144 ppm | 128 ppm | 114 ppm | 70 ppm | 46 ppm | 42 ppm | 31 ppm | 26 ppm | 10 ppm |
| 0 | | 0.68 | 0.57 | 0.61 | 0.62 | 0.60 | | 0.69 | 0.62 | | |
| 30 | 0.94 | 0.91 | 0.92 | 0.91 | 0.89 | 0.91 | 0.91 | 0.87 | 0.88 | 0.88 | 0.94 |
| 50 | 1.11 | ND | ND | ND | ND | 1.13 | 1.22 | 1.18 | 1.21 | 1.21 | 1.19 |
| 70 | 1.72 | ND | ND | ND | ND | 1.72 | 1.69 | 1.69 | ND | 1.69 | 1.75 |
| 100 | 2.64 | | | | | | 2.51 | | | 2.50 | 2.50 |

[a] The accuracy of the measurements is ±5%. ND stands for not detected due to low signal-to-noise ratio.

implies that it is the best contact time for PEOx. For Phenoxy, the best contact time is within 1−1.5 ms.[25] As a compromise, the contact time used in all the NMR experiments for this system is 1.5 ms.

In the $T_1(H)$ experiment, the resonance intensities of pure Phenoxy, pure PEOx and their blends were obtained with a series of different delay times. On the basis of the inversion recovery mode employed in this experiment, the $T_1(H)$ can be calculated from the following exponential equation

$$M_\tau = M_e\left[1 - 2\exp\left(\frac{-\tau}{T_1(H)}\right)\right] \quad (1)$$

where $T_1(H)$ is the proton spin−lattice relaxation time in the laboratory frame, $\tau$ is the delay time used in the experiment, $M_\tau$ is the resonance intensity at delay time $\tau$, and $M_e$ is the resonance intensity at $\tau \geq 5T_1(H)$. By rearranging eq 1 and taking natural logarithm on both sides, the following equation can be obtained:

$$\ln\left[\frac{(M_e - M_\tau)}{(2M_e)}\right] = \frac{-\tau}{T_1(H)} \quad (2)$$

By plotting $\ln[(M_e - M_\tau)/2M_e]$ vs $\tau$, $T_1(H)$ can be obtained from the slope.

Figure 8 shows the logarithmic plot of $^{13}C$ resonance intensity $M_\tau$ vs delay time $\tau$ for the selected carbon (10 ppm) of pure PEOx and Phenoxy/PEOx blends. It is found that the fitting of the experiment data with the single exponential decay function is quite good at the entire selected delay time range and only one straight line is obtained for each composition. The $T_1(H)$ values obtained from eq 4 for all resonance carbons in pure Phenoxy, pure PEOx, and their blends are summarized in Table 2. Single $T_1(H)$ decays were obtained for all the blends, and the $T_1(H)$ values of all carbon resonances remained the same within experimental error. This means that the spin-diffusion among all protons in this blend can average out the whole relaxation process and hence the domain size of this blend is smaller than the spin-diffusion path length within the time $T_1(H)$. For complete averaging over the time of relaxation, the upper limit of the domain size can be estimated from the calculation of the average diffusion path length by using the following equation[26−28]

$$L = [6DT_i(H)]^{1/2} \quad (3)$$

where $T_i(H)$ is the relaxation time ($T_1(H)$ or $T_{1\rho}(H)$), corresponding to the relaxation experiment, and $D$ is the effective spin-diffusion coefficient which depends on the dipolar interaction and the average distance between protons. Typically, $D$ is on the order of $10^{-16}$ $m^2$ $s^{-1}$, and for the $T_{1\rho}(H)$ experiment, $D$ is half of this value. From the measured values of $T_1(H)$ and eq 3, it

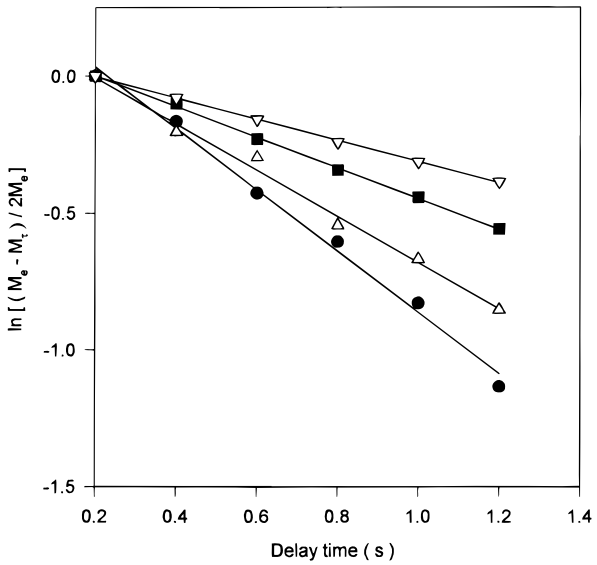


**Figure 8.** Logarithmic plot of resonance intensity (at 10 ppm) vs delay time to measure $T_1(H)$. Phenoxy/PEOx: 0/100 (▽); 30/70(■); 50/50 (△); 70/30 (●).

is estimated that the Phenoxy/PEOx blends are intimately mixed on a scale less than 200−300 Å.

The spin-diffusion process can further be characterized by the spin−lattice relaxation time in the rotating frame $T_{1\rho}(H)$ in which the homogeneity of polymer blends can be examined on a smaller scale. In the $T_{1\rho}(H)$ experiment, the spin-locking mode was employed, and the magnetization of resonance is expected to decay according to the following exponential function model:

$$M_\tau = M_0\exp\left(\frac{-\tau}{T_{1\rho}(H)}\right) \quad (4)$$

Rearranging eq 4 and then taking the natural logarithm on both sides, we have

$$\ln\left(\frac{M_\tau}{M_0}\right) = \frac{-\tau}{T_{1\rho}(H)} \quad (5)$$

where $M_0$ is the initial magnetization. If $\ln[(M_\tau/M_0)$ is plotted vs $\tau$, $T_{1\rho}(H)$ can be obtained from the slope.

Figure 9 shows the logarithmic plot of $^{13}C$ resonance intensity $M_\tau$ vs delay time $\tau$ for the selected carbon (10 ppm) of pure PEOx and Phenoxy/PEOx blends. It is clear that the experimental data fits eq 5 quite well, and a straight line is obtained for each composition. Furthermore, it can be seen that from Table 3, a single $T_{1\rho}(H)$ was obtained for both pure components and blends and the obtained $T_{1\rho}(H)$ values can be considered to be the same within experimental error. All these imply that all the blends are homogeneous even on the $T_{1\rho}(H)$ sensitive scale of 10−15 Å, according to eq 3.

**Table 3. $T_{1\rho}(H)$ Values (ms) for Phenoxy, PEOx, and Their Blends[a]**

| composition | PEOx | Phenoxy (PH) | | | | | PEOx | PH | | PEOx | |
|---|---|---|---|---|---|---|---|---|---|---|---|
| (PEOx wt %) | 174 ppm | 157 ppm | 144 ppm | 128 ppm | 114 ppm | 70 ppm | 46 ppm | 42 ppm | 31 ppm | 26 ppm | 10 ppm |
| 0 | | 2.72 | 2.87 | 2.84 | 2.63 | 2.95 | | 2.86 | 2.77 | | |
| 30 | 5.49 | 5.28 | 5.30 | 5.38 | 4.75 | 4.67 | ND | 5.48 | 5.47 | 5.59 | 5.50 |
| 50 | 5.95 | 5.66 | ND | ND | ND | ND | 5.88 | 5.88 | 5.72 | 5.77 | 5.56 |
| 70 | 7.53 | ND | ND | ND | ND | ND | 7.53 | 7.26 | 6.91 | 7.10 | 7.03 |
| 100 | 4.02 | | | | | | 4.03 | | | 3.79 | 4.05 |

[a] The accuracy of the measurements is ±5%. ND stands for not detected due to low signal-to-noise ratio.

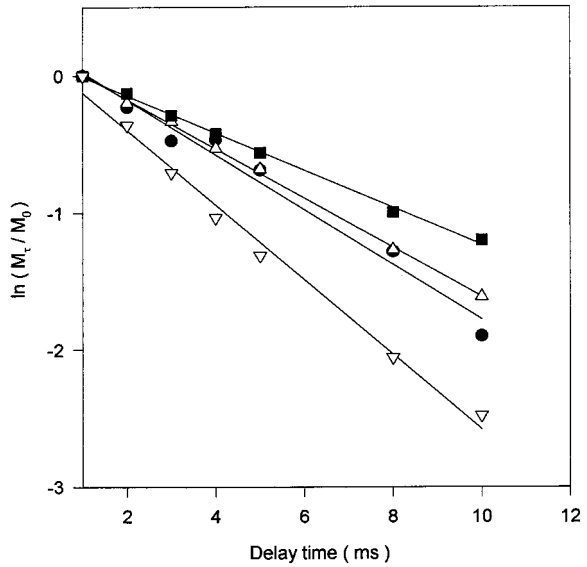


**Figure 9.** Logarithmic plot of resonance intensity (at 10 ppm) vs delay time to measure $T_{1\rho}(H)$. Phenoxy/PEOx: 0/100 (▽); 30/70 (■); 50/50 (△); 70/30 (●).

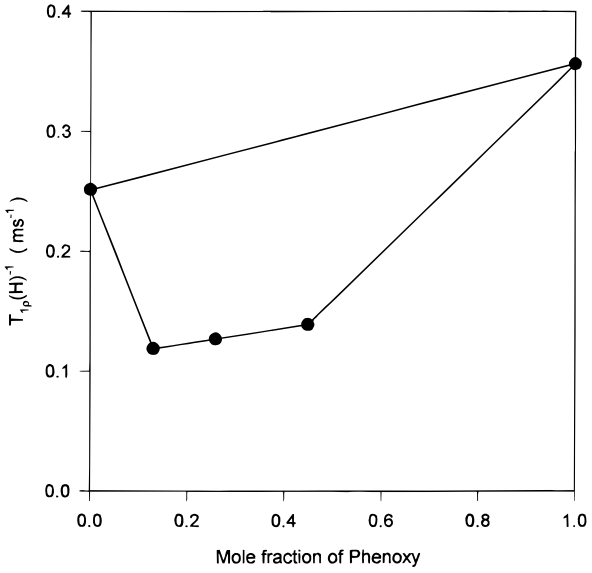


**Figure 10.** Plot of $T_{1\rho}(H)^{-1}$ calculated from eq 6 vs composition.

The average proton relaxation rate (the inverse of the relaxation time) of a homogeneous blend can be predicted by the model for linear additivity of relaxation rates for pure components[29−31]

$$\frac{1}{T_i(H)} = \left(\frac{N_A M_A}{N_T}\right)\left(\frac{1}{T_i(H)_A}\right) + \left(\frac{N_B M_B}{N_T}\right)\left(\frac{1}{T_i(H)_B}\right) \quad (6)$$

where $1/T_1(H)_A$ and $1/T_1(H)_B$ denote the relaxation rates of pure components A and B, respectively; $N_A$ and $N_B$ are the numbers of protons per mole of the respective components, $M_A$ and $M_B$ are the mole fractions of the components, and $N_T = N_A M_A + N_B M_B$.

The proton relaxation rates, $1/T_{1\rho}(H)$, calculated from eq 6, are plotted vs mole fraction of Phenoxy in Figure 10. It can be seen that for each composition, the calculated relaxation rate deviates significantly from the composition average line. This result indicates that the blending of Phenoxy with PEOx alters the state of segmental motion of their components significantly due to strong hydrogen bonding and thus induces the longer $T_{1\rho}(H)$ values obtained in the blends as compared with those of the pure components. Therefore, the $T_{1\rho}(H)$ values of the blends do not lie intermediate between those of the pure components.

## Conclusions

The homogeneity of the Phenoxy/PEOx is achieved due to the formation of the intermolecular hydrogen bonding. For the measurements of spin−lattice relaxation times in both laboratory and rotating frame, single values of $T_1(H)$ and $T_{1\rho}(H)$ were obtained and the data can be best-fitted by the single-exponential decay function for each composition. Moreover, the values of all carbon resonances can be considered the same within experimental error. All these reveal that Phenoxy/PEOx blends exhibit homogeneous amorphous phase over the entire composition range and intimate mixing occurs no larger than 10−15 Å scale.

**Acknowledgment.** This work was supported by the Croucher Foundation Grant (CF 95/96.EG 04).

## References and Notes

(1) Olabisi, O.; Robeson, L. M.; Shaw, M. T. *Polymer−Polymer Miscibility*; Academic Press: New York, 1979.
(2) Utracki, L. A. *Polymer Alloy and Blends*; Hanser Publishers: Munich, Germany, 1989.
(3) McBrierty, V. J.; Packer, K. J. *Nuclear Magnetic Resonance in Solid Polymer*; Cambridge University Press: Cambridge, U.K., 1993.
(4) Mathias, L. J., Ed. *Solid State NMR of Polymer*; Plenum Press: New York, 1991.
(5) Coleman, M. M.; Graf, J. F.; Painter, P. C. *Specific Interaction and the Miscibility of Polymer Blends*; Technomic Publishing Inc.: Lancaster, PA., 1991.
(6) Brode, G. J.; Koleske, J. V. *J. Macromol. Sci.* **1972**, *6*, 1109.
(7) Robeson, L. M.; Furtek, A. B. *J. Appl. Polym. Sci.* **1979**, *23*, 645.
(8) Robeson, L. M.; Furtek, A. B. *J. Am. Chem. Soc., Div. Org. Coat. Plastics Chem.* **1977**, *37*, 136.
(9) Seymour, K. W.; Zehner, B. E. *J. Polym. Sci., Polym. Phys. Ed.* **1980**, *18*, 2299.
(10) Yuan, Y. M.; Ruckenstein, E. *Polymer* **1998**, *39*, 1893.
(11) Yuan, Y. M.; Ruckenstein, E. *J. Appl. Polym. Sci.* **1998**, *67*, 913.
(12) Wu, H. D.; Chu, P. P.; Ma, C. M. *Polymer* **1998**, *39*, 703.
(13) Dai, J.; Goh, S. H.; Lee, S. Y.; Siow, K. S. *Polymer* **1996**, *37*, 3259.
(14) Lichkus, A. M.; Painter, P. C.; Coleman, M. M. *Macromolecules* **1988**, *21*, 2636.

(15) Meaurio, E.; Cesteros, L.; Katime, I. *Macromolecules* **1997**, *30*, 4567.
(16) Meaurio, E.; Velda, J. L.; Cesteros, L.; Katime, I. *Macromolecules* **1996**, *29*, 4598.
(17) Schmulbach, C. D.; Drago, R. S. *J. Phys. Chem.* **1960**, *64*, 1956.
(18) Bull, W. E.; Madan, S. K.; Willis, J. E. *Inorg. Chem.* **1963**, *2*, 303.
(19) Chalapathi, V. V.; Ramiah, K. V. *Curr. Sci.* **1968**, *16*, 453.
(20) Zheng, S.; Mi, Y.; Guo, Q. *J. Polym. Sci., Polym. Phys.*, in press.
(21) Zhang, X.; Takegoshi, K.; Hikichi, K. *Polymer* **1992**, *33*, 712.
(22) Qin, C.; Priesm, A. T. N.; Belfiore, L. A. *Polym. Commun.* **1990**, *31*, 177.
(23) Miyoshi, T.; Takegoshi, K.; Hikichi, K. *Polymer* **1997**, *38*, 2315.
(24) Gobbi, G. C.; Silvestri, R.; Russell, T. P.; Lyerla, J. R.; Fleming, W. W.; Nishi, T. J. *Polym, Sci, Polym. Lett. Ed.* **1987**, *25*, 61.
(25) Diehl, P.; Fluck, E.; Gunther, H.; Kosfeld, R.; Seelig, J. *Solid-State NMR III: Organic Matter*; Springer-Verlag: Berlin, 1994.
(26) McBrierty, V. J.; Douglass, D. C. *J. Polym. Sci. Macromol. Rev.* **1981**, *16*, 295.
(27) Demco, D. E.; Johannsson, A.; Tegenfeldt, J. *Solid State Nucl. Magn. Reson.* **1995**, *4*, 13.
(28) Clauss, J.; Schmidr-Rohr, K.; Spiess, H. W. *Acta Polym.* **1993**, *44*, 1.
(29) McBriety, V. J.; Douglass, D. C.; Kwei, T. W. *Macromolecules* **1978**, *11*, 1265.
(30) Douglass, D. C. Polymer Characterization by ESR and NMR; ACS Symbosium Series 142; American Chemical Society: Washington DC, 1980.
(31) Dickson, L. C.; Yang, H.; Chu, C. W.; Stein, R. S.; Chien, J. C. W. *Macromolecules* **1987**, *20*, 1757.
(32) Kaplan, D. S. *J. Appl. Polym. Sci.* **1976**, *20*, 2615.

MA980714I